Radiating effect of participating media in a flameless industrial reactor

Giuliano Cammarata, Giuseppe Petrone
Department of Industrial and Mechanical Engineering,
University of Catania
Viale A. Doria, 6 - 95125 Catania, Italy
gcamma@diim.unict.it, gpetrone@diim.unict.it

ABSTRACT

A 3D multi-physical numerical model concerning fluid-dynamical and thermo-chemical behaviour of a flameless reactor is presented in this communication. The analysed industrial device exploits a recent combustion technique that seems to largely hinder thermal NO_x formation. Modelling and computations are carried-out by using a multi-physical FEM commercial software. The swirling jet used for combustive injection is firstly analysed, then the entire reactor volume is considered for simulations. The fluid-dynamics of the process is based on a k-ε turbulence model, coupled with four diffusion-transport equations whose the first one characterises the temperature, while the remaining three are related to the concentrations of the chemical species involving in the process. In order to consider the radiating effects of participating media inside the combustion chamber, the Rosseland approximation is invoked in solving the energy equation. Results principally highlight the occurrence of a Reverse Flow Zone closed to the inlet section of the swirling injection system and a flat temperature profile characterising thermal distribution throughout the control volume of the reactor. These findings are in good agreement with experimental data concerning similar operating devices.

1. INTRODUCTION

The opportunity of improving combustion efficiency and reducing harmful emissions represents one of the major goal for energy systems in which an oxidation process occurs. For that reason, a special attention is paid since several years both by basic researchers and design engineers in new combustion technologies for industrial burners. NO_x emissions represent a relevant and dangerous pollutant for environment. Because of its formation mechanism, exploiting air nitrogen and oxygen, NO_x emissions are produced even when a cleaned fuel is used for combustion. There are three predominant mechanisms of NO_x formation during a combustion process, prompt NO_x, fuel NO_x and thermal NO_x, respectively. Thermal NO_x is the mean mechanism at high temperature, so that the most common NO_x-reducing techniques used for combustion systems (flame cooling, staged-combustion, lean premixed combustion, …) are based on the possibility of cutting off peaks of temperature. Recently, innovative high temperature air combustion techniques were proposed in order to develop energy-efficient and environment-friendly combustion devices [1]. Originally, this kind of

technology was named as Excess Enthalpy Combustion. Its various developments are today named as High temperature Air Combustion (HiTAC), Flameless Oxidation (FLOX), Low NOx Injection (LNI) or Mild Combustion (MILD) [2]. An exhaustive review concerning the state of art of the above techniques was recently published by Cavaliere et al. [3].

In flameless oxidation technique, the feeding of oxidising agent and fuel gas is performed separately (extreme staging of combustion) with high injection speeds [4]. The functional principle of this mode of combustion consists in using a diluted mixing of high preheating incoming fluids with exhaust inert gases before burning. For dilution we mean that combustive and fuel are locally mixed with exhaust gases before burning. A common way to operate consists in re-circulating exhaust gases close to the nozzle of the burner. Usually, the geometrical shape of the burner, as well as the high speeds of the inlet flows, determinates large internal re-circulations of the combustion products inside the control volume of reaction. The most used kind of injection system for combustive consists in swirling jets or bluff-body air injection systems.

Swirling jets are used as a means of controlling flames in combustion chambers [5]. The aerodynamics of swirling turbulent jets combine the characteristics of rotating-motion and the free turbulence phenomena encountered in jets and wake flows. When rotating motion is imparted to a flow upstream a nozzle, it assumes a main tangential velocity component in addition with the axial and radial ones. The tangential component of velocity induces the flow in changing its direction, so that a spiral form is set up. Then, a low pressure zone in the central core of this spiral, characterized by annular vortexes, is set up. This phenomenon is called Processing Vortex Core (PVC). The physical appearance of the PVC in swirling flames reduces the flame length and generates a high emissivity flame. In presence of a strong degree of swirl, the radial and, above all, the axial pressure gradients, associated with the PVC, results in the setting up of a “Reverse Flow Zone” (RFZ) along the burner axis, characterized by an internal flow recirculation. The RFZ allows to recycle heat and active chemical species to the root of the flame, providing a stable flame itself with a good performance for a number of carboneous materials which are usually difficult to burn. Thus, an efficient combustion takes place, characterized by a stable flame and a reduced percentage of emissions (particularly NOx) [6].

From a thermal point of view, the high temperature of the re-circulated combustion products is used to initiate and maintain the oxidation reaction. In flameless applications, the luminescence of flame can no longer be seen and combustion is, for the most part, distributed throughout the volume of the combustion chamber. This is why this combustion mode is called flameless combustion. If oxidising agent is pure oxygen, the concentration of nitrogen inside the reactor is strongly reduced if compared to the atmospheric standard, obtaining low emission of NO_x although the high temperatures maintained in the combustion chamber. While in the conventional burners the forehead of flame is characterized by high gradients (there is almost a discontinuity in chemical composition and temperature between reagents and products), in the flameless mode combustion involves the whole volume of the combustion chamber [1].

It is known that in many high-temperature applications, the medium between surfaces is not transparent, but it absorbs and emits radiation over the infrared range of wavelength [7]. In typical combustion process two mechanisms principally contribute in this physical behaviour, banded radiation in the infrared spectrum due to emission and absorption by molecular gaseous combustion products and continuum radiation due to tiny burning soot particles or other suspended particles [8]. However, the calculation of heat transfer rate due to radiation in an enclosure filled by participating media is an argument of not easy solution. Spectral radiative properties of the most common gaseous encountered as combustion product

(mainly a mixing of CO_2 and H_2O) have been largely studied and despite of this are actually subject of ongoing research [9, 10, 11, 12, 13, 14]. On the other hand, the influence of suspended particulate shape, and its state of aggregation, on radiative heat transfer of soot-containing combustion products is an argument of present interest for several researchers [15, 16].

From a practical point of view, the presence of a mixture of semi-opaque gases (tri-atomic molecules) and soot clouds generates a strong radiating field inside the volume of a furnace. In application with high temperature, radiation becomes the predominant way of heat exchange, more than convection. As result of strong heat flux in thermal exchange overall the combustion chamber, an homogeneous temperature distribution (flat profile), avoiding peaks of temperature, is commonly detected in experimental or operating industrial devices exploiting the discussed mode of combustion.

Despite the high scientific, environmental and industrial interest concerning the possibility of applying in large scale this combustion technique, due to its recent development no many studies have been yet done. Some experimental results have been published [2, 17] while a very few numerical studies are actually available in literature [18]. In order to contribute in developing of this favourable technology, a numerical investigation on fluid-dynamical, chemical and thermal processes involving in functioning of industrial reactors exploiting this technology is presented in this study. For the studied system thermo-physical properties of processing fluids, needed for solving fluid-dynamics, are temperature dependent. Thermal convection and transport of chemical species depend on velocity field while in energy equation the source term, expressed as chemical reaction enthalpy, is function of the concentration gradient of combustion product (where reaction takes place energy is produced). For the above discussed reasons, a multi-physical approach was necessary in order to completely describe the system.

This article is divided into three main sections concerning fluid-dynamics, diffusion and transport of chemical species and thermal analysis, respectively. In order to be more easily readable, modelling and results are sequentially illustrated and discussed in each section. However, it is to notice that, because of coupling of governing equations, the above mentioned “several physics” were simultaneously simulated.

2. SWIRLING JET INJECTION SYSTEM AND FLUID-DYNAMICS OF ENTIRE REACTOR

The first step presented in this study illustrates the fluid-dynamics of the swirling jet injection system for incoming combustive. In most of the combustion applications, swirl burners are usually of simple geometrical shape, even if the aerodynamics is very complex due to the high levels of turbulence [6]. Methods of generating swirling jets are several:tangential inlet of the fluid stream into a cylindrical duct, rotation of mechanical devices which confer a swirling motion to the fluid flowing trough them or use of “guide vanes” in an axial flow. The swirl intensity can be quantified, with good approximation, by an experimental parameter S, called “swirl number”. It is defined as the ratio between the axial flux of the angular momentum, and the axial flux of axial momentum multiplied for the exit radius of the burner nozzle. Experimental analyses have shown as varying swirl number, the Reverse Flow Zone presents different degrees of recirculation. It is so possible to establish the following classification [19]:

- “Weak” swirl (S<0.6), the pressure gradients are not large enough to generate a recirculation zone;
- “Medium” swirl (0.6<S<1), a light recirculation zone is generated, due to larger axial pressure gradients;

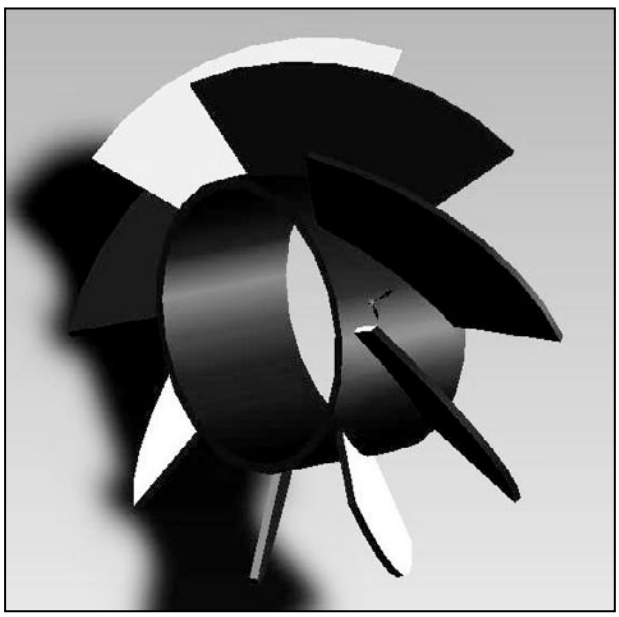

Figure 1 Geometrical model of the swirler.

- "Strong" swirl (S>1), a very large recirculation zone is generated, due to the high pressure gradients developed in the core.

For the studied swirl burner the degree of swirl belongs to the "medium" class, and the swirl effect is generated by guided vanes. The geometrical model of the "swirler" has been realized apart by CAD software (Figure 1) and then imported into the drawing grid of the FEM software used for simulations, i.e. COMSOL Multiphysics version 3.2.

The geometrical model is divided into two different parts (Figure 2). The first, where the axial swirler is located, represents the final part of the burner, while the second represents the initial part of the combustion reactor. Considering a Newtonian fluid and an incompressible turbulent flow (Ma<<1, Re>>2000), the fluid dynamical analysis is based on a k-ε model of the flow. Momentum and mass conservation equations read in steady state as in following:

$$\left(U\cdot\nabla\right)U = {-\nabla p}\big/{\rho} + \nabla\cdot\left[\left(\nu+\nu_T\right)\nabla U\right]$$

$$\nabla\cdot U = 0$$

where density of fluid has been considered as a linear function of temperature. Then, two closure equations are needed to solve the problem:

$$\left(U\cdot\nabla\right)k = \tau_{ij}\frac{\partial u_i}{\partial x_j} - \varepsilon + \nabla\cdot\left[\left(\nu+\frac{\nu_T}{\sigma_k}\right)\nabla k\right]$$

$$\left(U\cdot\nabla\right)\varepsilon = c_{\varepsilon 1}{\varepsilon}\big/{k}\cdot\tau_{ij}\frac{\partial u_i}{\partial x_j} - c_{\varepsilon 1}{\varepsilon^2}\big/{k} + \nabla\cdot\left[\left(\nu+\frac{\nu_T}{\sigma_\varepsilon}\right)\nabla\varepsilon\right]$$

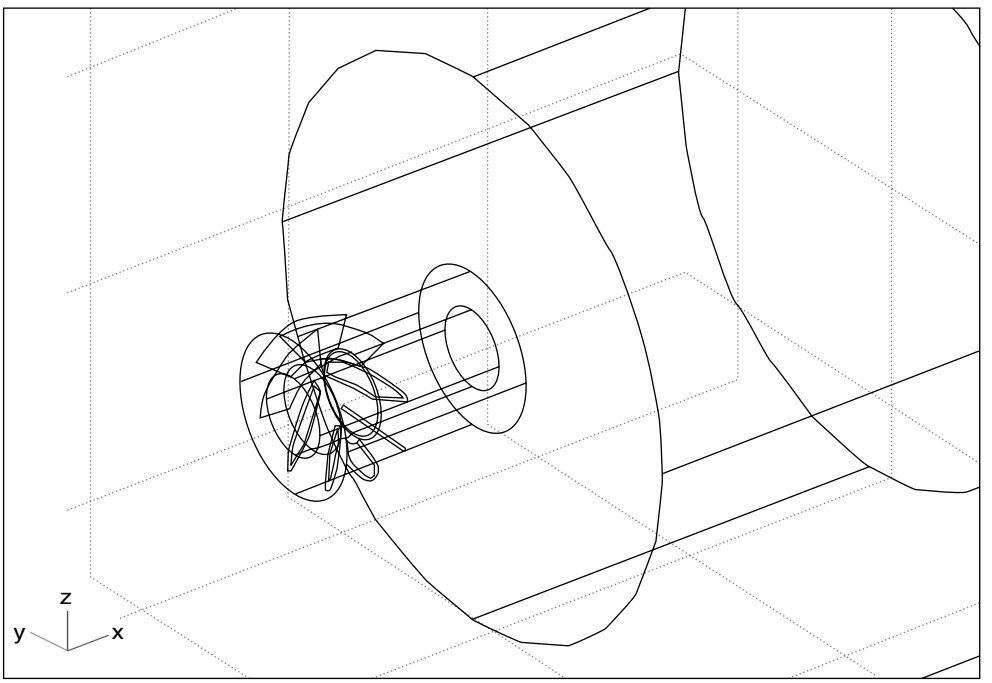

Figure 2 Geometrical model of the injection system.

where $c_{\tau 1}$ and $c_{\tau 2}$ are constant and k and ε represent the kinetic turbulent energy and the dissipative turbulent energy, respectively.

These differential equations are numerically integrated with the following boundary conditions: combustive enters the collar inlet duct with an average axial velocity of *20 m/s*, no-slip conditions are set on the walls and a pressure equal to *3 bar* is considered on the last frontal section. The above set of partial differential equations with boundary conditions is discretized on a no-structured computational grid made of tetrahedral elements, finer close to the swirler zone. The degrees of freedom for the analysed system are about 500,000. The linear system have been solved by the UMFPACK method on a 64 bit dual-core processor with 16 Gb of RAM.

The obtained results are now discussed. Figure 3 shows velocity fields evaluated in a longitudinal section of the reactor.

It is possible to observe as in the first duct the fluid accelerates when it goes trough the swirler. Further, when fluid enters into the reactor, it expands itself (with the classical cone course) and velocity field assumes values of about *2-3 m/s*. Then, from the velocity streamlines analysis, is easy to observe the spiral motion imparted to the fluid by the swirler (Figure 4), typical of swirling jets.

As previously described, the pressure gradients in the spiral core region result in the setting up of the RFZ. This is well represented in Figure 5 where the axial velocity isosurfaces are plotted. The bulb, located in the central core, corresponds to negative values of axial velocity. That means the fluid is recirculated toward the burner outlet section. The same results are reported in Figure 6, where the axial velocity is plotted as a function of the geometry radius. The negative values of axial velocity reflect the central core recirculation close to the burner outlet (continuous line). Although, RFZ keeps his intensity until the

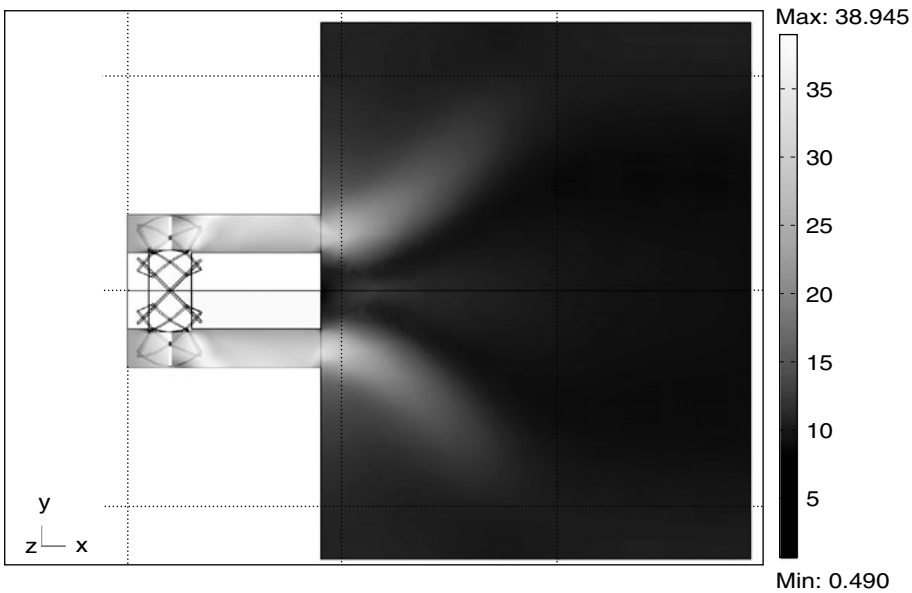

Figure 3 Velocity field in a longitudinal section of the model.

distance from it is quite a long away. In fact, the dashed and dotted-dashed lines show as velocity still assume negative values in the core up to about *20 cm*. Analyzing these values, the RFZ results stronger close to the burner outlet and, then, it decreases as soon as the fluid reaches the reactor central zone.

The obtained results qualitatively show a good correspondence with those coming from literature [19]. The swirl number of the examined device, evaluated adopting an analytical expression based on experimental studies, results equal to 0.77. Then, it belongs to the "medium swirl" class, characterized by pressure gradients enough for the RFZ development. Thus, the recirculation effects reported by the numerical model reflect the real swirl burner behaviour. At the same time, pressure field has been analyzed, too. It also has found correspondence with literature predictions. Particularly, a strong depression in the central core is detected, that confirms one more time the RFZ development. In a second step of the present study fluid-dynamics of the entire reactor has been considered. The governing equations correspond with those reported above, boundary conditions are also unchanged, except for the imposed pressure condition applied this time on the outlet section of the entire reactor. On the other hand, the injection system results modified in order to keep into account the inlet of two different fluids, fuel and combustive, respectively. Due to too much high computational cost, in the global model of the reactor, no bladed collar with guided vanes were considered and a simple annular inlet duct allow the combustive to enter the reaction volume. Nevertheless, the high speed of fluid particles incoming trough the injection channel generates a very important level of turbulence inside the reactor.

3. DIFFUSION AND TRANSPORT OF CHEMICAL SPECIES

This section is devoted to the analysis of chemical reactions occurring inside the reactor. Two fluid components enter the reaction volume, combustive and fuel, respectively. From a basic

Figure 4 Streamlines of flow.

point of view, we can assume that the above mentioned incoming fluids react for giving as product a third component, i.e. the combustion product. Due to the presence of three chemically heterogeneous components, three conservation equations are needed to describe the chemical diffusion and convection of the process. The governing equations, in their steady form, can be written as in following:

$$\nabla \cdot (D \nabla c_i) = R - U \cdot \nabla c_i \qquad i \in \{1,2,3\}$$

where D is the diffusion coefficient while c_i represent the concentration of oxidation agent, fuel and combustion product, respectively. Kinetics of chemical reactions is expressed in the source term R. In the present model, the reaction rate R is set equal to zero in the inlet sub-domains of the reactor, while it assumes the expression $R = \pm f_R c_1^2 c_2$ in the main cylindrical control volume. Algebraic sign of the reaction factor is set negative for c_1 and c_2 components (reacting agents), while it is positive for the c_3 component (combustion product). The reaction factor f_R is set equal to *1e-1*. Transport-diffusion equations are solved giving initial concentrations for incoming fluids at inlet sections. These values are imposed as a fraction between density at inlet temperature and molecular mass of the chemical agents. In particular, for the fuel an initial concentration of *527 mol/m³* is imposed, while for the oxidation agent we consider a concentration of *34.48 mol/m³*. All other surfaces are considered impermeable, except for the outlet section where outgoing concentration fluxes are imposed.

Results are now presented and discussed. The occurrence of a total mixing of the reacting fluids is confirmed by the analysis of the distributions of concentration for the chemical species involving in the process. In Figure 7 molar fraction of chemical species are reported

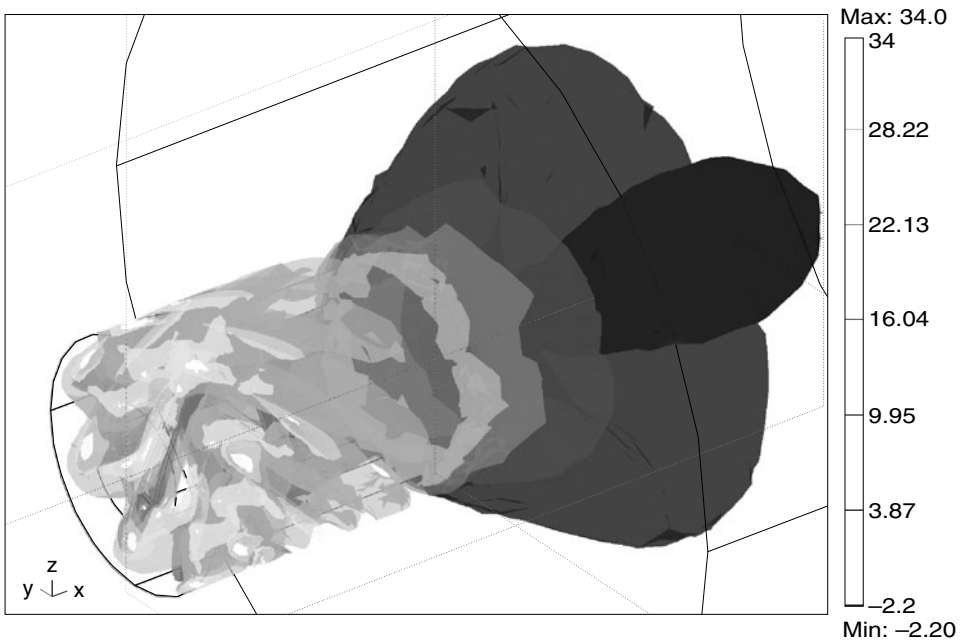

Figure 5 Isosurfaces of axial velocity.

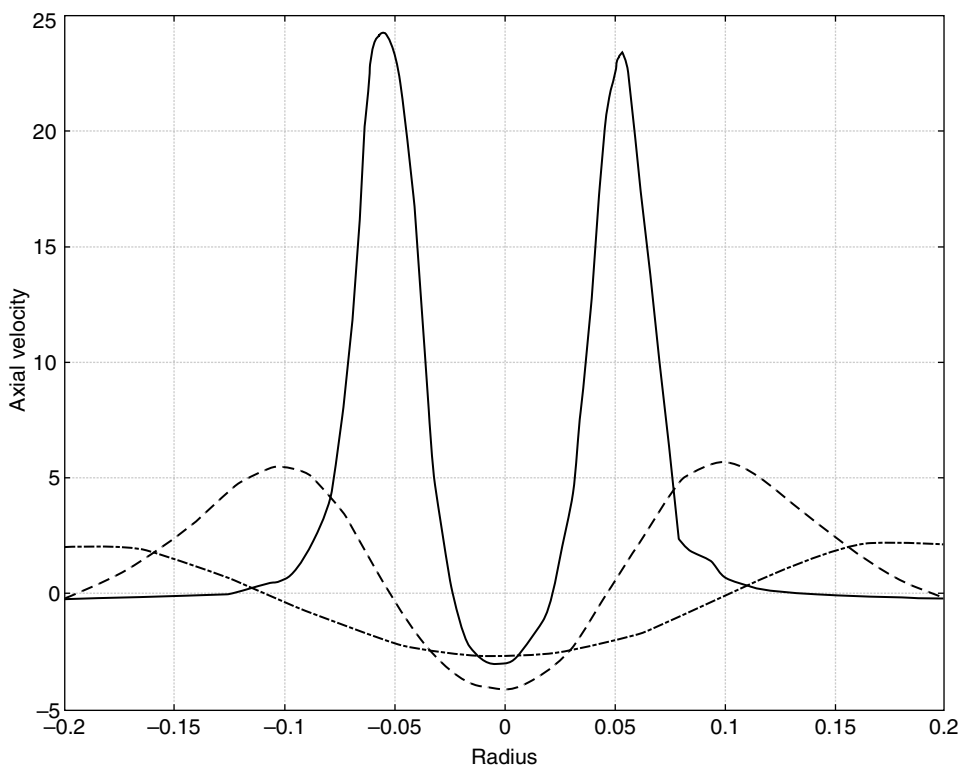

Figure 6 Radial distribution of axial velocity close to the burner outlet (continuous line), long away 10 cm (dashed line) and 20 cm (dotted-dashed line) from it.

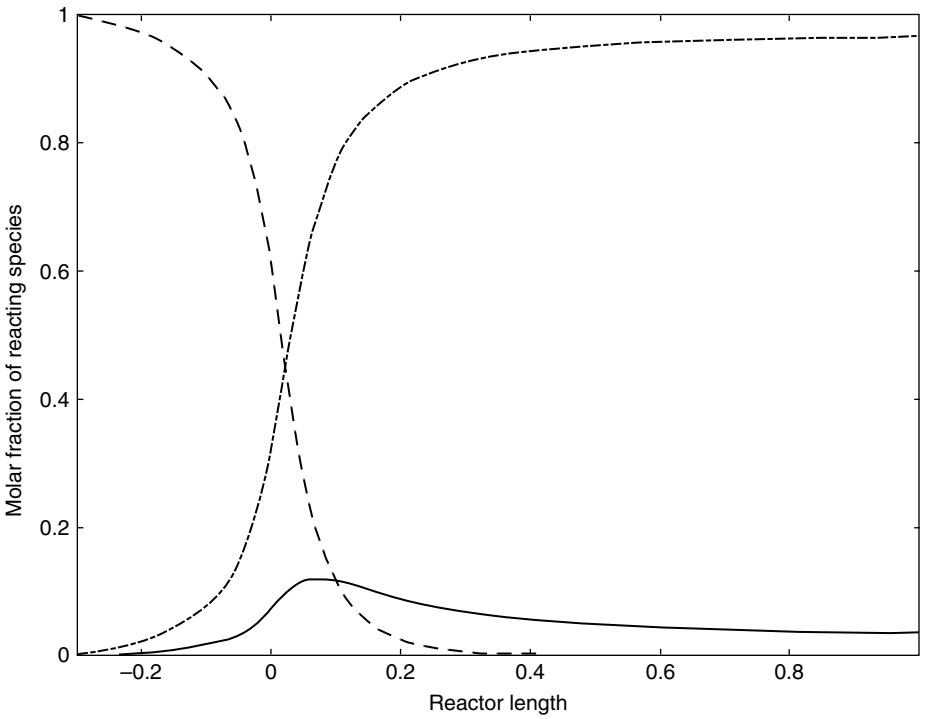

Figure 7 Molar fraction for reaction product (continuous line), fuel (dashed line) and combustive (dashed-dotted line) as a function of the reactor axial length.

as function of the axial length of the reactor. As can be observed, a peak of molar fraction for reaction product is detected close to inlet section for incoming fluids, then it becomes almost constant until the end of the combustion chamber. On the other hand, fuel concentration decreases along the inlet channel from its beginning value (*527 mole/m*^{3}) to about *32 mole/m*^{3}.

Then, this value quickly reaches zero when fluid incomes inside the control volume of the reactor, just in the proximity of the end of the inlet channel. This item underlines that no unburned residuals are produced in the process, with the consequently opportunity of having an high level of combustion efficiency for the considered system. Because of molar fraction of chemical species are plotted in Figure 7 with respect to the geometrical longitudinal axis of the reactor, concentration of oxidising agent results very low until the zero value of the abscise axis of the diagram. In fact inlet of this component is made trough the annular duct, concentric with respect to the longitudinal axis of the geometry. However, it is to notice that oxidising agent is present with high concentration along the entire cylindrical control volume of the combustion chamber. This behaviour reflects the operative conditions for a flameless combustion modality.

In fact, a flameless combustion process is characterized by a gradual oxidation in the totality of the combustor control volume. This is assured by the dilution in high temperature semi-inert gases (incoming fresh air or pure oxygen mixed with re-circulated exhaust gases) of the fuel introduced in the combustion chamber. In Figure 8 we present concentration isosurfaces for the reaction product. The trigging zone of the chemical reaction is clearly visible. The maximum value of concentration is observed very close to the end of the inlet channels where combustive and fuel meet each other and where oxidation principally takes

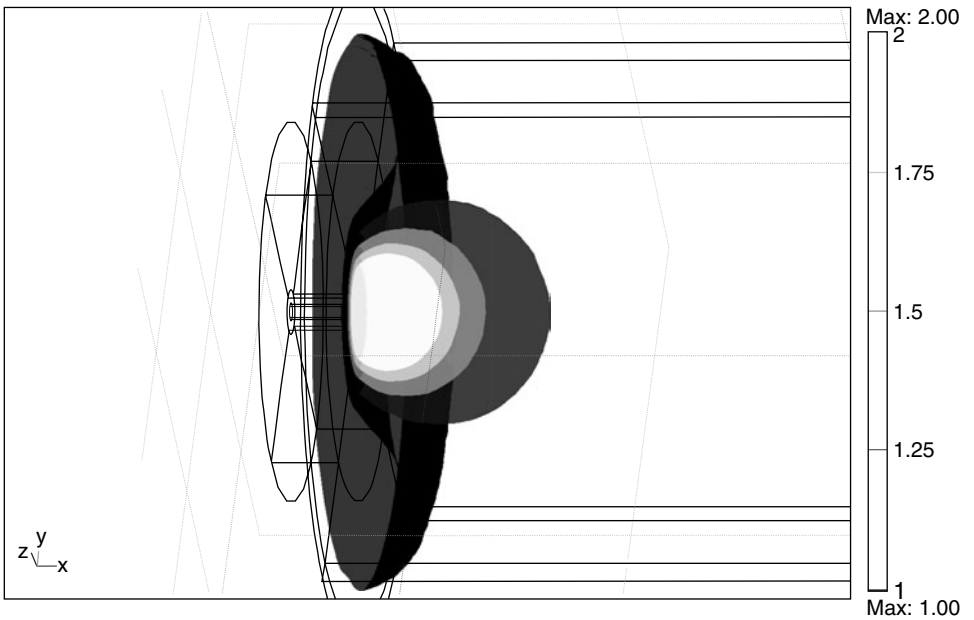

Figure 8 Isosurfaces of concentration for reaction product.

place. The chemical reaction is seen to be very fast in the space and the concentration gradient of the reaction product also reaches its maximum value in this portion of the combustion chamber.

4. THERMAL ANALYSIS

In the present section thermal behaviour of the analysed device is presented. Neglecting the dissipative term, the steady energy balance assumes the following expression:

$$\rho c_p U \cdot \nabla T = \nabla \cdot (k_c \nabla T) + \nabla \cdot q^r + S_T$$

where convective term is expressed in the first member of the equation, while the conductive one is reported as first term in the second member. Let now focus our attention on the source term, named as S_T in the above equation. This term is for sure dependent by the calorific power characteristic of the considered fuel. For the present study we considered a fuel with a calorific power $Hi \approx 4.11e7\ J/kg$. However, in order to correlate heat generation with combustion chemical reaction, the source term S_T has been expressed as function of the concentration gradient of reaction product also. This procedure allows to keep into account two important items. From a spatial point of view, energy is effectively generated where chemical reaction takes place. From a quantitatively point of view, its total amount depends on the quantity of fuel transformed in reaction product. Indeed, the source term in the energy equation well represents the reaction enthalpy characterizing the oxidation reaction.

As preliminary introduced in this article, one of the functional principles of the flameless oxidation technology consists in the occurrence of a strong radiating field inside the combustion chamber, generated by the semi-opaque participating medium. In fact, since the reaction was trigged, the radiating flux enables the maintaining of a gradual oxidation of reacting agents throughout the total volume of the furnace. In order to simulate this thermal

behaviour, a special attention was paid in dealing with radiative term in energy equation. Indeed, the medium inside the reactor is not transparent, but it is absorbing and emitting. In a typical combustion process this interaction results in two main mechanisms. The first one is related to the banded radiation in the infrared due to emission/absorption by molecular gaseous combustion products (mostly CO_2, H_2O). The second one is related to the continuum radiation due to tiny burning soot particles (coal particles, oil droplets or fly ash) present inside the combustion chamber. Concerning the first mechanism, it is known that the absorption/emission coefficient ε_λ for molecular gases is strongly dependent on wavelength. Gases tend to be transparent over most of the spectrum, but may be almost opaque over the spectral range of a band. However, for engineering applications it is often needed to determinate a total emissivity (over all spectrum of wavelength) of a mixture of several gases for an isothermal path. The total emissivity of a gas mixture could be evaluated and it is function of several factors as isothermal path length, gas temperature, partial pressure of absorbing gases and total pressure of mixture. According to the literature [8], for mixture of nitrogen with water vapour and carbon dioxide (most common combustion applications), the total emissivity may be calculated. For the present system it assumes the value $\varepsilon_{gas} \approx 0.4$. Concerning the second mechanism, since soot particles are very small (*0.005 m* to *0.08 m*) they are generally at the same temperature of the combustion gases and therefore strongly emit thermal radiation in a continuous spectrum over the infrared region. Experiments have shown that soot emission is stronger than the emission from the combustion gases. Mean absorption coefficient (κ_m) and emissivity for soot clouds may be also calculated. For the present system their values are $\kappa_m \approx 0.0916$ and $\varepsilon_{soot} = 1\text{-}e^{\kappa mL} \approx 0.6$. Since the molecular gases tend to emit only over a small part of the spectrum, with a little upper estimation, due to overlapping over some wavelength values, we can assume that the total emissivity of the mixture of gases and soot particulates corresponds to the sum of their single emissivity. For the studied system this assumption conduces to a global total emissivity for the medium evolving in combustion chamber $\varepsilon_{mix} = 0.9998$. In order to estimate heat transfer in participating media, under the assumption of optically thick medium the diffusion or Rosseland approximation can be invoked. A medium through which a photon can only travel a short distance without being absorbed, is known as optically thick medium. The optical thickness of a medium consists in the product of the absorption coefficient and a characteristic isothermal path length for the thermal system. If a medium is optically thick (optical thickness much higher than one), then the spectral radiative flux may be expressed as [7]:

$$q_\lambda^r = \frac{4}{3\kappa_\lambda} \nabla E_{b\lambda}$$

And integrating over all spectrum of wavelength, it becomes an equivalent diffusion term:

$$q^r = \frac{4}{3\kappa_R} \nabla E_b = \frac{4}{3\kappa_R} \nabla(\sigma T^4) = \frac{16\sigma T^3}{3\kappa_R} \nabla T = k_R \nabla T$$

Indeed, the radiative term can be expressed as an equivalent diffusive term and consequently the energy equation can be re-written as in following:

$$\rho c_p U \cdot \nabla T = \nabla \cdot (k_{gl} \nabla T) + S_T$$

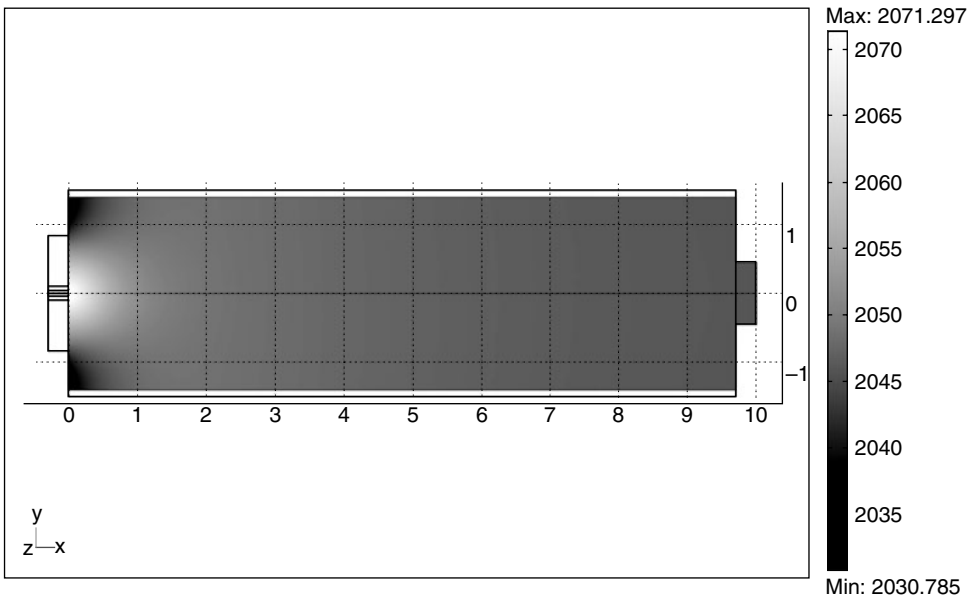

Figure 9 Temperature field in a longitudinal section of the reactor.

where a global conductivity $k_{gl} = k_c + k_R$ is introduced. The global conductivity keeps into account both real conductive and equivalent radiative terms. The parameter k_R is named as Rosseland mean absorption coefficient. For the studied system the radiative properties of the medium well satisfies the criterion of optically thick medium ($\kappa_m^{mix} L \approx 8.495$), so that the diffusion approximation was adopted in solving energy equation. Some preliminary tests have been conduced in order to validate this approach. In particular, the results of the diffusion approximation for participating media applied to a simplified 2D model of the discussed reactor have been compared with those obtained by using a P-N method. Otherwise, for the two employed methods, two different solvers were used for testing the validity of the diffusion approximation. Globally, comparisons showed good agreement between different methods and solving tools adopted.

Finally, energy equation was solved with the following boundary conditions: fixed temperatures for incoming fluids ($T = 723\ K$ for oxidising agent and $T = 423\ K$ for fuel), constant cooling flux for the external walls and outgoing heat flux for the outlet cross section of the reactor. The Figure 9 shows a longitudinal section of the reactor where thermal fields are reported. As expected, the maximum value in temperature ($T \approx 2070\ K$) occurs very close to the inlet ducts.

This simulated value well agrees with the theoretical value of the adiabatic flame temperature analytically evaluated for the considered fuel ($T_f \approx 2084\ K$). The local peak of temperature is extended along *1m* of axial length about, as better illustrated in Figure 10 where isosurfaces of temperature in the left portion of the reactor are reported. Then, the temperature field underlines an almost isothermal behaviour of the reactor. The almost constant value of temperature is $T \approx 2045\ K$. This value is in accordance with those experimentally detected for similar and actually operating reactors.

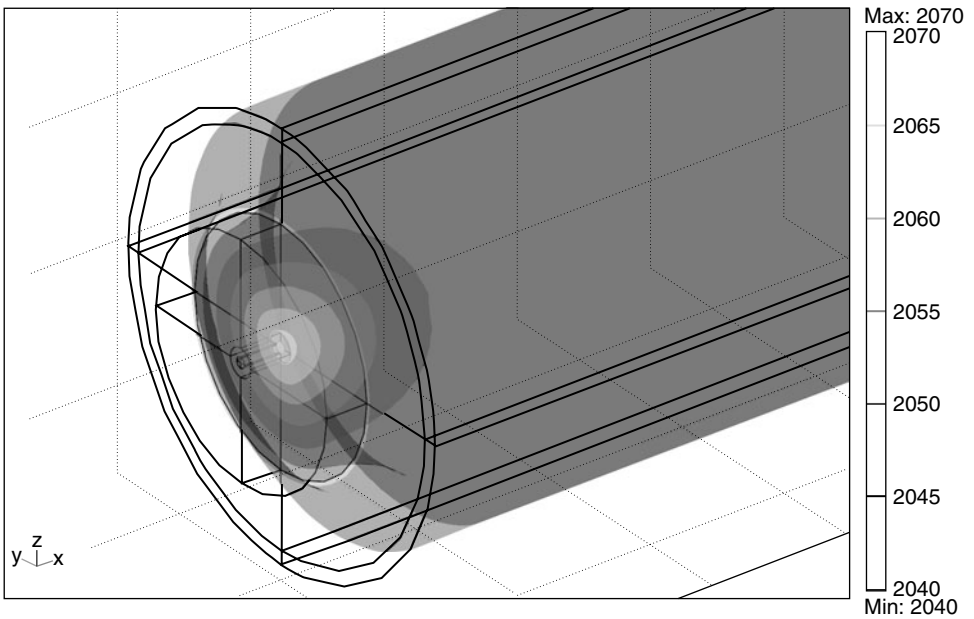

Figure 10 Isosurfaces of temperature in the left portion of the reactor.

5. CONCLUSION

A multi-physical 3D numerical analysis concerning fluid-dynamical, chemical and thermal behaviour of an industrial reactor exploiting the innovative "flameless oxidation" technology has been performed. Simulations of swirling jet injection system reflect with good approximation the real behaviour of the system. In particular the establishment of a Recirculation Flow Zone, characterized by negative values of the axial component of the velocity of fluid, close to its inlet section, has been highlighted. The reaction enthalpy generated by chemical process inside the control volume of the reactor has been evaluated and correlated with the heat source term in the energy equation. A numerical thermal model, based on the assumption of optical thick medium, has been implemented in order to keep in consideration the radiating heat exchanges related to the semi-opaque medium being inside the reactor. The obtained results show a flat temperature field occurring inside the cylindrical furnace. This thermal distribution also finds a good agreement with experimental data of operating similar devices. The present study clearly underlines the needed of simulating simultaneously several interconnected aspects of physics for technological systems, in order to completely describe their operative conditions.

REFERENCES

[1] Wunning J. A., Wunning J. G., Flameless oxidation to reduce thermal NO-formation, *Progress in Energy and Combustion Science*, 1997, Vol. 23, pp. 81–94.

[2] Weber R., Smart J. P., vd Kamp W., On the (MILD) combustion of gaseous, liquid, and solid fuels in high temperature preheated air, *Proceedings of the Combustion Institute*, 2005, Vol. 30, pp. 2623–2629.

[3] Cavaliere A., de Joannon M., Mild Combustion, *Progress in Energy and Combustion Science*, 2004, Vol. 30, pp. 329–366.

[4] Flamme M., Low NO_x combustion technologies for high temperature applications, *Energy Conversion & Management*, 2001, Vol. 42, pp. 1919–1935.

[5] Hillemans R., Lenze B., Leuchel W., Flame stabilisation and turbulent exchange in strongly swirling natural gas flames, Proceeding of the 21st International Symposium of Combustion, 1986.

[6] Fick W., O'Doherty T., Griffiths A. J., Syred N., Thermal characterization of Swirl burners, Proceeding of Energy and environment towards the year 2000, 1996.

[7] Siegel R., Howell J. R., *Thermal radiation Heat Transfer*, 3rd edition, Hemisphere, New York, 1992.

[8] Modest M. F., *Radiative Heat Transfer*, McGraw-Hill, New York, 1993.

[9] Kim O. J., Song T. H., Data base of WSGGM-based spectral model for radiation properties of combustion products, *Journal of Quantitative Spectroscopy & Radiative Transfer*, 2000, Vol. 64, pp. 379–394.

[10] Soufiani A., Taine J., High temperature gas radiative property parameters of statistical narrow-band model for H_2O, CO_2 and CO, and correlated-K model for H_2O and CO_2, *International Journal of Heat and Mass Transfer*, 1997, Vol. 40, pp. 987–991.

[11] Riviere PH., Langlois S., Soufiani A., Taine J., An approximate data base of H2O infrared lines for high temperature applications at low resolution. Statistical narrow-band model parameters, *Journal of Quantitative Spectroscopy & Radiative Transfer*, 1995, Vol. 53, pp. 221–234.

[12] Wang A., Modest M. F., High-accuracy, compact database of narrow-band k-distributions for water vapor and carbon dioxide, *Journal of Quantitative Spectroscopy & Radiative Transfer*, 2005, Vol. 93, pp. 245–261.

[13] Perez P., Boischot A., Ibgui L., Roblin A., A spectroscopic database for vapour adapted to spectral properties at high temperature, and moderate resolution, *Journal of Quantitative Spectroscopy & Radiative Transfer*, 2007, Vol. 103, pp. 231–244.

[14] Khan Y. U., Lawson D. A., Tucker R. J., Simple models of spectral radiative properties of carbon dioxide, *International Journal of Heat and Mass Transfer*, 1997, Vol. 40, pp. 3581–3593.

[15] Farias T. L., Carvalho M. G., Koylu U. O., Radiative heat transfer in soot-containing combustion systems with aggregation, *International Journal of Heat and Mass Transfer*, 1998, Vol. 41, pp. 2581–2587.

[16] Widmann J. F., Yang J. C., Smith T. J., Manzello S. L., Mulholland G. W., Measurement of the optical extinction coefficients of post-flame soot in the infrared, *Combustion and Flame*, 2003, Vol. 134, pp. 119–129.

[17] Choi G.-M., Katsuki M., Advanced low NO_x combustion using preheated air, *Energy Conversion & Management*, 2001, Vol. 42, pp. 639–652.

[18] Coelho P. J., Peters N., Numerical simulation of a mild combustion burner, *Combustion and Flame*, 2001, Vol. 124, pp. 503–518.

[19] Solero G., Experimental characterization of the isothermal mixing process in a model of a natural gas swirl combustor, Proceedings of the 50th ATI Congress, 1995.